Multifunctional nanoliposomes with curcumin–lipid derivative and brain targeting functionality with potential applications for Alzheimer disease

ARTICLE *in* EUROPEAN JOURNAL OF MEDICINAL CHEMISTRY · APRIL 2014

Impact Factor: 3.45 · DOI: 10.1016/j.ejmech.2014.04.050 · Source: PubMed

European Journal of Medicinal Chemistry 80 (2014) 175–183

Contents lists available at ScienceDirect

European Journal of Medicinal Chemistry

journal homepage: http://www.elsevier.com/locate/ejmech

Original article

Multifunctional nanoliposomes with curcumin–lipid derivative and brain targeting functionality with potential applications for Alzheimer disease

Spyridon Mourtas [a], Adina N. Lazar [b,c], Eleni Markoutsa [a], Charles Duyckaerts [b,c], Sophia G. Antimisiaris [a,d,*]

[a] Laboratory of Pharmaceutical Technology, Dept. of Pharmacy, School of Health Sciences, University of Patras, Rio 26510, Greece
[b] Laboratoire de Neuropathologie Escourolle, Hôpital de la Salpêtrière, AP-HP, 47 Bd de l'hôpital 75013 Paris, France
[c] Centre de recherche de l'ICM, (UPMC, INSERM UMR S 975, CNRS UMR 7225), 47 Bd de l'hôpital, 75013 Paris, France
[d] Institute of Chemical Engineering Sciences, FORTH/ICES, Rio, 26504 Patras, Greece

ARTICLE INFO

Article history:
Received 20 December 2013
Received in revised form
15 April 2014
Accepted 15 April 2014
Available online 18 April 2014

Keywords:
Curcumin
Amyloid
Targeting
Liposome
Nanoparticle
Multifunctional

ABSTRACT

With the objective to formulate multifunctional nanosized liposomes to target amyloid deposits in Alzheimer Disease (AD) brains, a lipid–PEG–curcumin derivative was synthesized and characterized. Multifunctional liposomes incorporating the curcumin derivative and additionally decorated with a Blood Brain Barrier (BBB) transport mediator (anti-Transferin antibody) were prepared and characterized. The fluorescence intensity of curcumin derivative was found to increase notably when the curcumin moiety was in the form of a diisopropylethylamine (DIPEA) salt. Both curcumin-derivative liposomes and curcumin-derivative Anti-TrF liposomes showed a high affinity for the amyloid deposits, on *post-mortem* brains samples of AD patients. The ability of both liposomes to delay Aβ1-42 peptide aggregation was confirmed by Thioflavin assay. However, the decoration of the curcumin-derivative liposomes with the Anti-TrF improved significantly the intake by the BBB cellular model. Results verify that the attachment of an antibody on the curcumin-liposome surface does not block deposit staining or prevention of Aβ aggregation, while the presence of the curcumin–PEG–lipid conjugate does not reduce their brain-targeting capability substantially, proving the potential of such multifunctional NLs for application in Alzheimer disease treatment and diagnosis.

1. Introduction

Alzheimer disease (AD) is the most common age related neurodegenerative disease, which is responsible for memory decline (initially) and widespread cognitive deficits (later) [1]. The main histopathological features of AD are extracellular aggregates of Aβ peptide in senile plaques and intraneuronal accumulations of tau protein and their detection in *post-mortem* tissue is requested for the diagnosis [2]. The initial event that leads to cortical dysfunction, in accordance to the "cascade hypothesis" [3], is the accumulation of Aβ peptides (most common fragments being the 40 and 42 amino acids peptides), produced by the cleavage of a large transmembrane type 1 protein (amyloid precursor protein, APP) [4–6]. The early detection of the amyloid deposits at an asymptomatic stage is still a challenge. Pittsburgh compound B (PIB) is the first radioligand that allowed *in vivo* detection and recording of the progression of Aβ pathology in the brain [7], however new probes are being developed with improved affinity for amyloid plaques.

Curcumin and different curcumin derivatives are able to bind to the amyloid deposits *in vivo*, *in vitro* or on *post-mortem* tissue, as shown by several studies [8–11]. The protective and curative properties of curcumin are well documented; according to *in vitro* studies, curcumin not only disrupts the aggregation of the amyloid peptide but is also able to disaggregate the already formed fibrils [12–14].

Nanoparticle-based delivery approaches have the potential to deliver therapeutic and/or imaging agents to the brain. Liposomes are such nanoparticles that are non-toxic, non-immunogenic, fully biodegradable, structurally versatile, and are among the most clinically recognized nanocarriers [15]. One of their major strengths

* Corresponding author. SGA: Lab Pharm Technology, Dept of Pharmacy, University Campus-Rio 1 & Foundation for Research and Technology – Hellas, Greece.
E-mail addresses: santimis@upatras.gr, santimis@hotmail.com (S.G. Antimisiaris).

http://dx.doi.org/10.1016/j.ejmech.2014.04.050
0223-5234/

is the ease of surface modification, which may be easily tailored according to their target [16]. Additionally, liposomes can be loaded with a variety of therapeutic and/or imaging agents due to the fact that they include aqueous and lipidic compartments. Their application as drug carriers for the CNS has been already demonstrated [17]. Recently the design and physicochemical characterisation of biocompatible curcumin-conjugated nanoliposomes (NLs) with high affinity for amyloid deposits, was reported [11,18]. Preliminary results indicate that such nanoliposomes could be used to design new probes, with diagnostic or therapeutic applications [11]. In order to reach the brain and, at a second step, the amyloid deposits, NLs should be able to pass across the blood–brain barrier (BBB). For this, multifunctional NLs bearing BBB transport mediators as well as the curcumin-derivative molecules (for amyloid deposit targeting), should be constructed. Main requirements for such multifunctional NLs to be able to pass the BBB and target the brain amyloid deposits, are: i) That they should be stealth (have the required blood circulation time in order to reach the BBB) and ii) That the addition of the BBB targeting ligand should not disturb their amyloid-targeting efficiency and vice-versa. In order to prepare such multifunctional NLs, a polyethylene glycol (PEG) coating is required to provide the stealth characteristics and to act as an anchoring point for BBB targeting ligands (as monoclonal antibodies). In this condition, the curcumin derivative on the NL surface should be placed at a distance from the vesicle bilayer, in order not to be "masked" by the PEG coating. Thereby, a new curcumin–lipid derivative was synthesized. In comparison to the previously studied curcumin–lipid derivative, the new one presents a PEG-spacer between the lipid and curcumin moiety. This novel lipid-PEG2000-curcumin (DPS-PEG2000-CURC) derivative was used for NL preparation; and these NLs were further characterized in regards to their affinity for amyloid deposits on *post-mortem* AD brains. After the additional immobilization of a BBB-transport mediator (monoclonal antibody [MAb]) on the constructed NLs, their potential as multifunctional NLs for AD applications was verified.

2. Experimental procedures

2.1. Materials

1,2-distearoyl-*sn*-glycero-3-phosphoethanolamine-N-[maleimide (polyethylene glycol) – 2000 (ammonium salt) [DSPE-PEG2000-MAL], and 1,2-distearoyl-sn-glycero-3-phosphocholine [DSPC], were from Avanti Polar Lipids (USA). Cholesterol [Chol], Fluorescein isothiocyanate–dextran 4000 [FITC-dextran], curcumin [CURC], and diisopropylethylamine [DIPEA], were from Sigma–Aldrich (purchased from Chemilab, Athens, Greece). All other chemicals, TLC plates and solvents, were from Merck (Germany). Anti-Transferin receptor monoclonal antibodies (Anti-TfR MAb), were from Serotec (clone OX26) and Bioledgend (clone RI1227).

2.2. Synthesis of DPS-PEG2000-CURC derivative (Schemes 1 and 2)

DSPE-PEG2000-MAL **(1)** (1mmole) was reacted with 4-methoxytritylthiol (Mmt-SH) (1.2 mmol) **(2)** in diisopropylethylamine (DIPEA) (2.6 mmol)/chloroform ($CHCl_3$) for 24 h at RT [19]. The reaction progress was monitored by TLC analysis until complete reaction of **(1)** (Scheme 1), and was subsequently subjected to flash chromatography using $CHCl_3$/methanol (MeOH) (6:1) as eluents. The collected fractions containing DSPE-PEG2000-S-Mmt product **(3)** were dried over P_2O_5 (80% yield). TLC analysis of the purified product gave one single UV and molybdenum blue spray positive spot (Rf = 0.43 in $CHCl_3$/MeOH 6:1) [20]. DPS-PEG2000-S-Mmt **(3)** was identified using ^{1}H NMR (400 MHz) and ESI-MS. In order to prepare the desired lipid-PEG2000-curcumin conjugate, DSPE-PEG2000-S-Mmt **(3)** was treated with 1% TFA (trifluoroacetic acid)/TES (triethylsilane) in dichloromethane (DCM) (95:5) to the corresponding free-thiol derivative DSPE-PEG2000-SH **(4)** (Scheme 1) which was subsequently condensed with methanol (MeOH) and then washed twice with Et_2O/Hex (2:1).

This gave **(4)** as an oily product of high purity (only one spot was detected –after I_2 and molybdenum spray application on TLC plate; Rf = 0.34 in $CHCl_3$/MeOH 6:1). The oily residue **(4)** was immediately used at the next step. Thus **(4)** (1 mmol) was dissolved in DCM/dimethylformamide (DMF) and DIPEA (7mmole), and curcumin (CURC) **(5)** (3 mmol) – dissolved in $CHCl_3$ – were slowly added (Scheme 2). The reaction progress was monitored with TLC until complete reaction of **(4)**, and then the reaction solvent was evaporated and the residual oil was re-suspended in $CHCl_3$. This was either purified directly with flash chromatography to afford **(6)** as a DIPEA salt, or further treated to afford **(6)** in its acid form. For this, the residual oil was acidified using 0.5% (v/v) aq.HCl (pH = 2–3) and the aqueous layers were extracted twice with $CHCl_3$. The combined organic layers were further washed with H_2O (twice) and finally dried over Na_2SO_4. The organic layer filtrates were purified using flash chromatography and the pure-product-containing-fractions were combined, evaporated and finally dried in vacuo over P_2O_5 to afford **(6)** in 60% yield (over the two steps). TLC analysis verified one single UV/Vis and Molybdenum blue spray positive spot (Rf = 0.32 in $CHCl_3$/MeOH 6:1) and the product was identified by ^{1}H NMR and ESI-MS.

2.3. DPS-PEG-CURC characterisation by NMR and ESI-MS

^{1}H NMR spectra were recorded at 293 K on a Brucker spectrometer 400 MHz using methanol-d4 (CD_3OD) as solvent and TMS as internal standard. Positive Electrospray mass spectra (ESI-MS) were performed with an electrospray platform (Waters) equipped with a Masslynx NT 2.3 operational system, using MeOH as solvent.

2.4. Preparation of nanoliposomes

NL's were prepared by the thin film hydration technique followed by sonication, as previously described [11,18]. In brief, the appropriate amount of lipids DSPC, Chol and DPS-PEG2000-CURC **(6)**, to give a final composition of DSPC/Chol/DPS-PEG2000-CURC equal to 2:1:0.375 – 0.75 (mol/mol/mol), were dissolved in $CHCl_3$/MeOH (2:1 v/v) and mixed in a round-bottom flask. The solvent was evaporated under vacuum until formation of a thin lipid layer on the walls of the flask and the lipid film was further treated with N_2 to remove organic solvent traces. The lipid was hydrated with PBS buffer (pH 7.4), or FITC-dextran (45 mg/ml) at 60 °C. After complete lipid hydration and formation of liposomes, the vesicle dispersion was placed under the microtip of a probe sonicator (Sonics & Materials) until it became completely clear. Minor Ti fragments were rejected by centrifugation and the clear supernatant (NL dispersion) was incubated for 1 h at 60 °C to anneal any structural defects. Lipid concentration in all liposome dispersions was routinely measured by the Stewart assay [21]. In the case of NLs which would be decorated with monoclonal antibody (MAb) ligands, at a second step, DSPE-PEG2000-MAL was also introduced in the liposome bilayer at 0.05 mol%, MAbs were ligated on the NL surface after applying a thiolation process, as described in detail elsewhere [22].

2.5. Characterisation of nanoliposomes

A Malvern nanosizer (particle sizer and ζ-potential analyser) was used for physicochemical characterization of NLs. Vesicle size

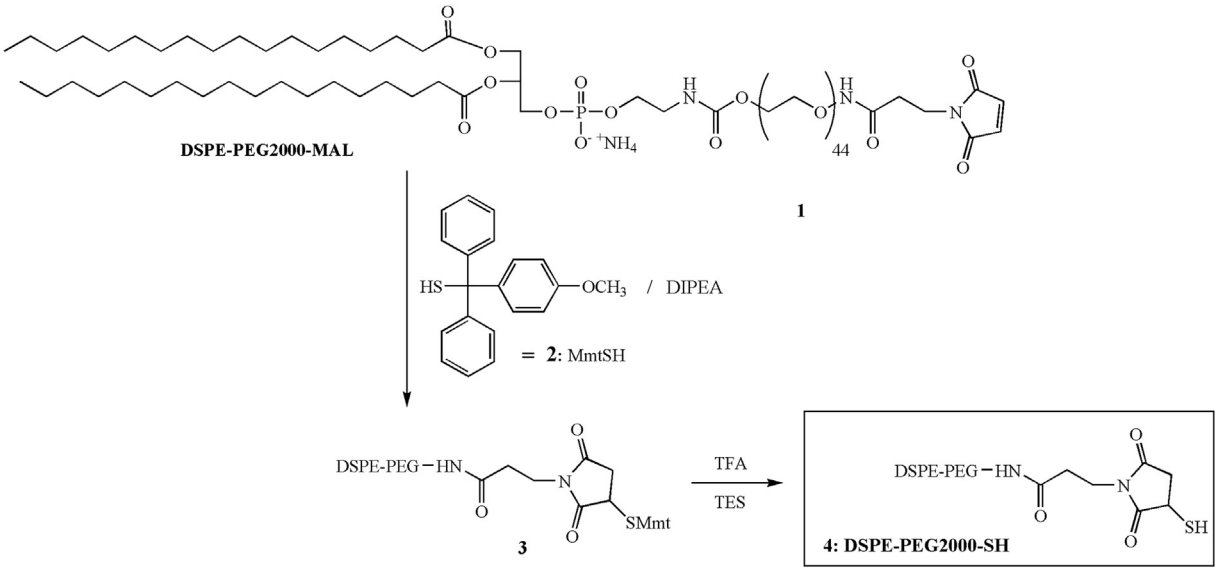

Scheme 1. Synthesis of DSPE-PEG2000-SH **(4).**

distribution was assessed by dynamic light scattering with a 625 nm laser beam, performed at 25 °C. The index of size and polydispersity were obtained from the intensity autocorrelation function of the light scattered at a fixed angle of 173° (conditions which avoid errors due to back-scattering). The ζ-potential was also measured at 25 °C.

2.6. Alzheimer disease cases

AD patients had been enrolled in a brain donation program of the Brain Bank "GIE NeuroCEB" run by a consortium of Patients Associations (including France Alzheimer Association) and declared to the Ministry of Research and Universities, as requested by French Law. An explicit consent had been signed by the patient himself, or by the next of kin, in accordance with the French Bioethical Laws. The corpse was transported to the mortuary of a University Hospital belonging to the NeuroCEB network, at the time of death and the brain was removed. One hemisphere randomly left or right, was fixed in buffered 4% formaldehyde for the neuropathological diagnosis of AD. The other hemisphere was immediately sliced. Samples from the superior temporal gyrus (Brodmann area 22), around 4 cm^3 in volume, were mounted on a cork piece with

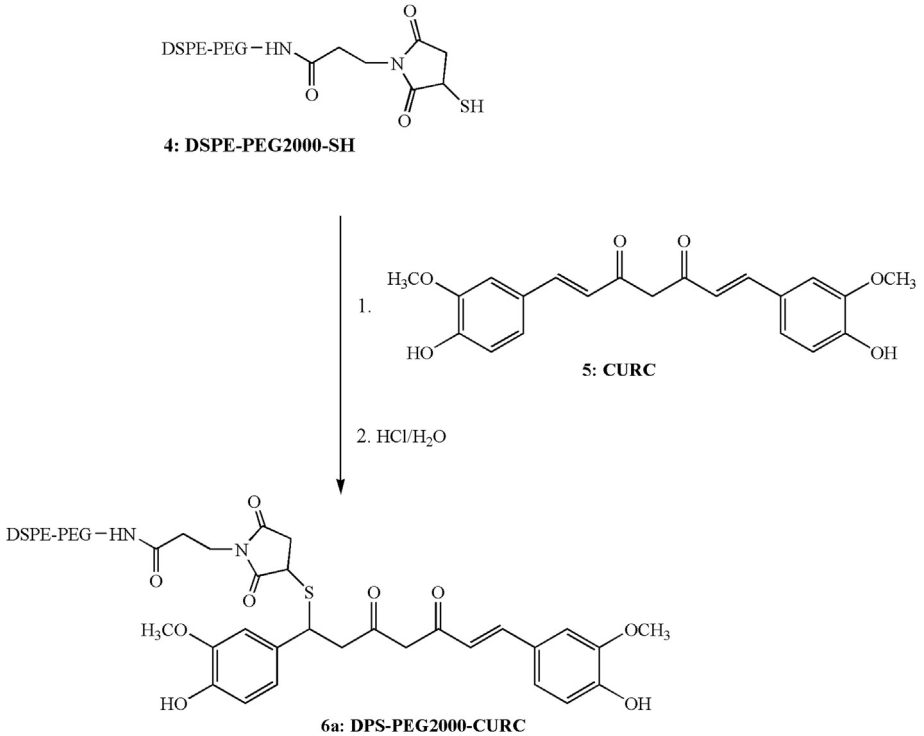

Scheme 2. Synthesis of DPS-PEG2000-CURC **(6)** from DSPE-PEG2000-SH **(4).**

Cryomount embedding medium and dipped in isopentane cooled by liquid nitrogen. The samples were kept in a deep freezer at −80 °C.

2.6.1. Diagnosis

Multiple formalin-fixed samples, including the hippocampus and isocortical Brodmann area 22, were embedded in paraffin, cut at a thickness of 5 μm and immunostained with anti-Aβ (6F/3D clone; Dako, Trappes France) and anti-tau (polyclonal rabbit anti-tau antibody; Dako; Trappes code number A 0024). The lesions were further staged according to Braak and Braak [23], and the density of the senile plaques (SPs) was evaluated according to the CERAD protocol [24]. The diagnosis criteria of the NIA-Reagan Institute were used [25].

2.6.2. Staining of AD tissues

Frozen samples from the temporal isocortex (superior temporal gyrus) and the hippocampus of three AD subjects (Braak neurofibrillary stage VI, Thal phase 5), containing numerous amyloid deposits were selected for the study. Sections of 10 μm thick were fixed for 10 min in 100% acetone washed three times for 5 min with PBS and incubated for 30 min with PBS-Tween 0.05% solution. They were further washed with PBS and incubated with a 200 μl suspension of liposomes, at 1/10, 1/50 and 1/100 dilutions, in PBS for 2 h. In the end, the samples were gently washed in PBS and mounted using a fluoromount medium (Dako). The tissue was examined using a Leica SP2 confocal microscope, at 488 nm excitation wavelength, and the signals were collected between 540 and 550 nm.

2.7. Aβ aggregation assays

The thioflavin T assay for oligomeric Aβ was performed using Aβ1-42 peptides that were de-seeded according to previously reported method [26]. This was achieved by dissolving 2 mg aliquot of recombinant Aβ1-42 (kindly provided by Mario Negri Institute, Milan, IT) in 0.5 ml trifluoroacetic acid containing 4.5% thioanisole, and kept on ice for 60 min. Peptide solution was mixed with 167 μl of pure, ice-cold formic acid, dropped onto ice-cold diethyl ether (1 ml), vortexed and kept for 20 min in an ice bath. After 15 min centrifugation at 13,000 rpm, peptides were collected at the bottom of the tube and carefully dissolved in H_2O:Acetonitrile 50:50 (v/v). The sample was divided into aliquots and lyophilized. Age reversed peptides were used immediately. Thioflavin T assays were conducted in 96-well, clear-bottomed microtitre plates, with 25 μM Aβ1-42, 15 μM thioflavin T, 40 μM liposome, in 10 mM PBS, pH 7.4, with a total reaction volume of 100 μl. Aggregation was monitored using a TECAN InfiniTE-M200 plate reader (λex = 450 nm, λem = 482 nm) over 96 h at 30 °C, with the plate being shaken and then read at 0, 4, 24, 48, 72 and 96 h.

2.8. Cell uptake studies

Immortalized human brain capillary endothelial cells (hCMEC/D3) (passage 25–35) were used [27]. The cell line was obtained under license from Institut national de la Sante et de la Recherche Medicale (INSERM, Paris, France). Cells were seeded at 27,000 cells/cm^2 and grown in EBM-2 medium (Lonza, Basel, Switzerland) supplemented with 10 mM HEPES, 1 ng/ml basic FGF (bFGF), 1.4 μM hydrocortisone, 5 μg/ml ascorbic acid, penicillin-streptomycin, chemically defined lipid concentrate, and 5% ultralow IgG FBS. The cells were cultured at 37 °C, 5% CO_2 and saturated humidity. All culturewares were coated with 0.1 mg/ml rat tail collagen type I (BD Biosciences). Medium was changed every 2–3 days.

For NL uptake by cells, FITC-dextran-encapsulating vesicles were incubated with confluent monolayers of hCMEC/D3 cells, as previously reported in detail [28]. In brief, 200 nmoles liposomal lipids were incubated with 10^6 cells in medium (containing 5% (v/v) FCS) at 37 °C, for 60 min, then washed in ice-cold PBS (×3), detached from plates, re-suspended in PBS and assayed for FITC FI (after cell lysis in 2% Triton X-100). Cell auto fluorescence was always subtracted.

3. Results

3.1. Confirmation of DPS-PEG-CURC conjugated lipid

DSPE-PEG2000-MAL **(1)**, DSPE-PEG2000-S-Mmt **(3)** and DPS-PEG2000-CURC **(6)** were subjected to ^{1}H NMR and ESI-MS analysis to prove the conversion of **(1)**, first to product **(3)** and then to product **(6)**. TLC analysis for both **(3)** and **(6)** showed the synthesis of highly purified products (one spot detected with UV–Vis, I_2, and molybdenum blue spray). ^{1}H NMR analysis of DSPE-PEG2000-S-Mmt **(3)** generally showed that maleimide protons of DSPE-PEG2000-MAL **(1)** at 6.83 ppm (see Supplementary Data Fig. S1, A) completely disappeared while methoxy (3.82 ppm) and aromatic (7.6–6.88 ppm) signals of the Mmt-group appeared (see Supplementary Data Fig. S1, B). ^{1}H NMR analysis of DSPE-PEG2000-CURC **(6)** showed the existence of two different methoxy signals at 3.90 and 3.94 ppm (see Supplementary Data Fig. S1, C) attributed to methoxy-groups of curcumin, while the ones at 7.7–6.7 ppm, to its aromatic and alkene protons. Since the integration of the protons in the aromatic moiety when attached to the high molecular weight PEG does not give accurate peak heights, as reported elsewhere [29.30], minor differences from the expected integration values in the aromatic region were fixed at the expected value.

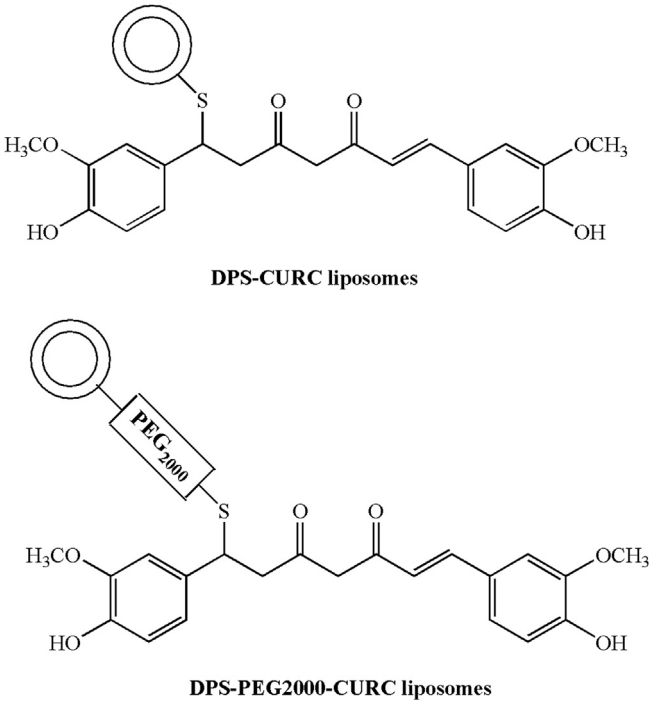

Fig. 1. Illustration of liposomes decorated with DPS-CURC and DPS-PEG2000-CURC **(6)** by the self-assembling of DPS-CURC and DPS-PEG2000-CURC within a liposome membrane.

Table 1
Physicochemical characteristics of the various types of NLs constructed. Each value is the mean of at least 3 different formulations and SD values of each mean are presented.

NL composition	Mean diameter (nm)	PDI	ζ-Pot (mV)	Yield (%) MAb
A: DSPC/Chol (2:1) + 10 mol% DPS-CURC	109.8 ± 5.7	0.195 ± 0.021	−2.01 ± 0.40	
B: DSPC/Chol (2:1) + 10 mol% DPS-PEG2000-CURC	116.1 ± 3.7	0.280 ± 0.018	−6.07 ± 0.47	
C: DSPC/Chol (2:1) + 20 mol% DPS-PEG2000-CURC	159.3 ± 2.1	0.206 ± 0.017	−7.43 ± 0.95	
D: DSPC/Chol (2:1) + 20 mol% DPS-PEG2000-CURC + 0.05 mol% MAb	153 ± 11	0.277 ± 0.014	−7.5 ± 1.2	62.5

Positive Electrospray mass spectra of products DSPE-PEG2000-S-Mmt **(3)** and DPS-PEG2000-CURC **(6)** dissolved in MeOH revealed an inverted U shape mass spectral pattern with an increment of 44 or (22 for +2, 14.67 for +3 and 11 for +4), characteristic for PEG-molecules, spanning between the expected molecular weights (See Supplementary Data, Fig S2).

3.2. Physicochemical properties of DPS-PEG2000-CURC NLs

The structure of DPS-PEG2000-CURC NLs and DPS-CURC NLs is illustrated in Fig. 1. As seen in Table 1, a slight increase of mean vesicle diameter (from 110 to 116 nm), polydispersity index (PI, a measure of size homogeneity), and zeta-potential is observed when DPS-PEG2000-CURC (B) is incorporated in NLs, compared to those incorporating DPS-CURC (A). This is justified by the fact that 10 mol % of PEG with a molecular weight of 2000 was attached to the liposome bilayer, with the CURC derivative. When the DPS-PEG2000-CURC content of the vesicles is increased from 10 mol% (B) to 20 mol% (C), their size increases even more (from 116 to 159 nm), a logical consequence since the amount of lipidic-CURC derivative incorporated in the vesicle bilayer, is double; however PI and zeta-potential values are not significantly affected. Furthermore, the decoration of the later vesicles (C) with a low amount (0.05 mol %) of anti-TfR-MAb does not have any significant effect on their physicochemical properties.

3.3. Labelling of amyloid deposits in post-mortem AD brains

In order to determine whether the novel DPS-PEG2000-CURC NLs presented affinity for amyloid deposits with respect to the DPS-CURC, we compared the ability of both NL-types (i.e. DPS-PEG2000-CURC and DPS-CURC NLs, Fig. 1) to label the senile plaques on *post-mortem* brain tissue of AD patients.

It was found that the novel liposomes (DPS-PEG2000-CURC NLs) abolished the high fluorescence previously observed with DPS-CURC liposomes [11], and stained the plaques very weakly (Fig. 2, A & B).

In order to understand this behaviour (low fluorescence labelling of amyloids), the participation of the two phenol-groups on the fluorescence of DPS-PEG2000-CURC **(6)** was explored, by taking into account their donating ability on the total resonance of the molecule. For this, DIPEA was added to a DPS-PEG2000-CURC-NL

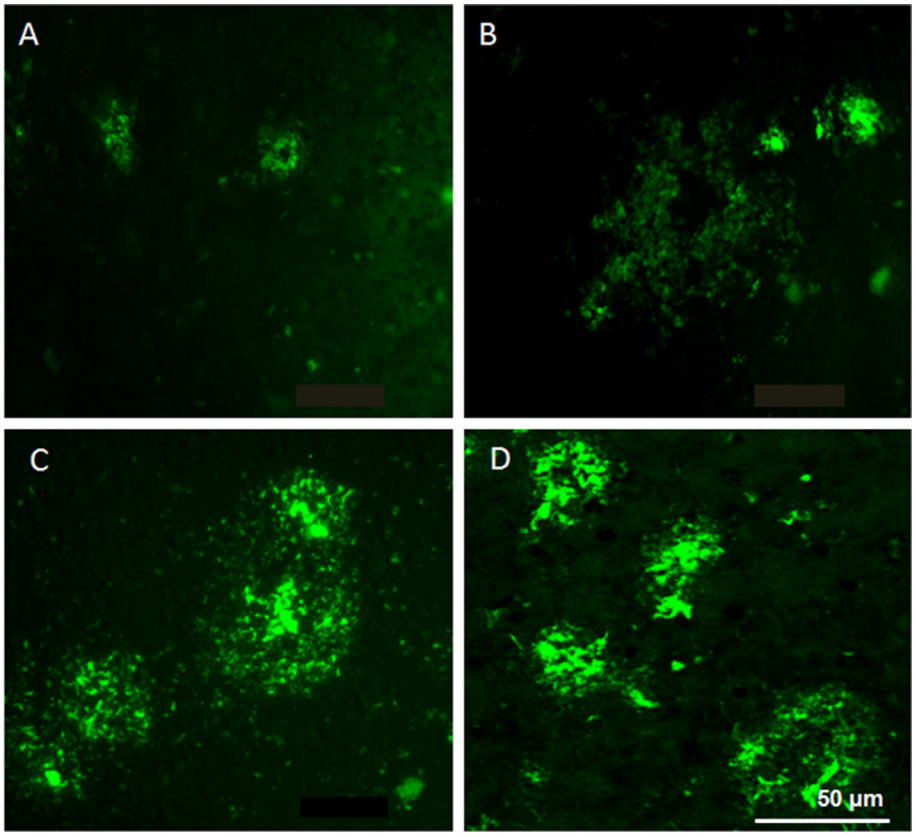

Fig. 2. Affinity of curcumin-liposomes for the amyloid deposits on AD brain tissue. A and B: labelling of the amyloid deposits by DPS-PEG2000-CURC (non-DIPEA salt) liposomes; C: labelling of the amyloid deposits by the DPS-PEG2000-CURC (DIPEA salt) liposomes; and D: labelling of the amyloid deposits by the antiTrF + DPS-PEG2000-CURC (DIPEA salt) liposomes.

Table 2
Fluorescence Intensity (FI) measurements of DPS-CURC vs. DPS-PEG2000-CURC **(6)** [both dissolved in MeOH]. Each sample was measured 5 times, $n = 3$, and mean values with SDs of the means are reported.

Compound	FI before DIPEA	FI after DIPEA
DPS-CURC (DIPEA salt)	18.04 ± 0.13	17.99 ± 0.12
DPS-PEG2000-CURC	3.251 ± 0.036	17.08 ± 0.12

and DPS-CURC-NL solution (in MeOH) and the Fluorescence Intensities (FI's) of the two compounds (DIPEA salt and acid) were measured at EX: 488 nm and EM: 545 nm. It was observed that, although the addition of DIPEA in DPS-CURC (DIPEA salt) solution did not affect its fluorescence, a high enhancement (almost 6 times) in FI value was demonstrated in the case of DPS-PEG2000-CURC (Table 2), revealing its conversion to the corresponding DIPEA salt, which is strongly improving the fluorescence (Scheme 3).

The ability of these improved DPS-PEG2000-CURC$_{(DIPEA)}$-NLs to efficiently label Aβ depositions was tested on *post-mortem* brain tissue of AD patients. A strong labelling of the senile plaques was observed (Fig. 2C). Furthermore, the additional decoration of the surface of DPS-PEG2000-CURC$_{(DIPEA)}$-NLs with a monoclonal antibody, in order to facilitate the passage though the blood–brain barrier did not affect their capacity to label the amyloid deposits Fig. 2D. Thus, the presence of the antibody on the surface of the NLs did not impede curcumin's affinity for the Aβ aggregates.

The colocalization of the DPS-PEG2000-CURC NLs fluorescence with the immunohistochemistry of an anti-Abeta antibody confirmed the specificity of the labelling for the senile plaques (Fig. 3).

3.4. Aβ peptide aggregation

It was previously reported that DPS-CURC NLs inhibit the aggregation of Aβ peptides [31]. In order to verify if they retain the later activity (retardation and decrease of abeta-peptide aggregation) after the PEG-moiety is incorporated between the lipid and CURC part of the CURC derivative, and also to evaluate if further decoration of the liposomes-surface with MAb's (to produce multifunctional NLs) blocks the previously reported activity of the NL-surface-immobilized CURC-derivative, DPS-PEG2000-CURC NLs together with MAb-decorated DPS-PEG2000-CURC NLs, and the corresponding control formulations were evaluated for their effect on Aβ peptide aggregation. DPS-PEG2000-CURC NLs (as DPS-CURC NLs) demonstrated a continuous inhibitory activity on Aβ-peptide aggregation, for the whole period of the study, as seen in Fig. 4. Indeed, the insertion of the PEG-chain in the DPS-CURC liposomes only slightly affected their ability to inhibit Aβ1-42 aggregation (significant differences between the relative aggregation values of DPS-CURC and DPS-PEG2000-CURC NLs were observed only at the 48 and 72 h points). Additionally, when a monoclonal antibody was immobilized on the DPS-PEG2000-CURC NLs their ability to inhibit Aβ-peptide aggregation was only slightly decreased, and Aβ-peptide aggregation was still substantially inhibited. It should be noted that although some inhibition of late-stage aggregation was also found with the control liposomes, this was not statistically significant (at any of the time points evaluated).

3.5. Uptake by BBB cellular model

As proven above, the activity of the CURC-derivative immobilized on the surface of the multifunctional NLs, was not substantially affected by the co-presence of the monoclonal antibody on their surface. Thus it was important to also investigate whether the CURC derivative modulates the brain-targeting capability of the anti-TfR MAb. For this, the uptake of such multifunctional NLs and corresponding NLs without the CURC-derivative (decorated only with MAb, at the same surface density) by hCMEC/D3 human brain endothelial cells, was measured. As seen in Fig. 5, the uptake values measured for control liposomes (without any surface-immobilized ligand), and those decorated with the MAb, are similar to those previously reported for the same NL types [32], verifying that the

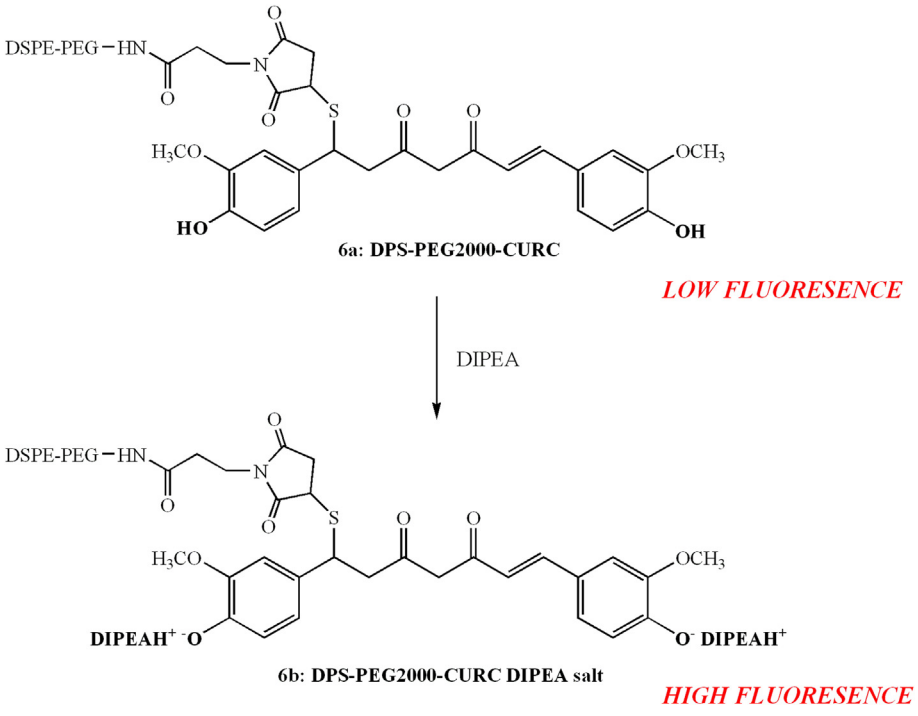

Scheme 3. DPS-PEG2000-CURC **(6)** in acidic form **(6a)** (low fluorescence) or as DIPEA salt **(6b)** (high fluorescence).

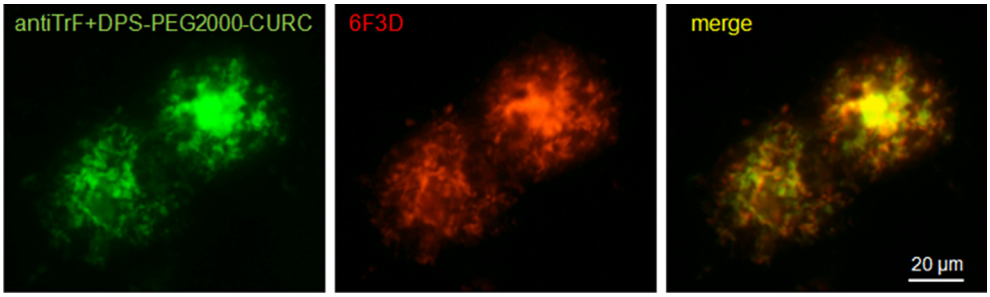

Fig. 3. Micrographs of antiTrF + DPS-PEG2000-CURC (DIPEA salt) liposomes (green) and 6F3D anti-Abeta antibody (red) double labelling on AD brain; the co-localization (yellow in the merge) demonstrated the specificity for the amyloid deposits. (For interpretation of the references to colour in this figure legend, the reader is referred to the web version of this article.)

study was carried out correctly. As demonstrated, there is only a very slight decrease (<10%) in the uptake for the MAb-decorated NLs which are concurrently decorated with the CURC-derivative (compared to those decorated only with the MAb), which verifies that the brain targeting potential of such multifunctional NLs is not substantially affected due the presence of the CURC-derivative on their surface.

4. Discussion

In a quest for a cheap, specific and sensitive marker for amyloid targeting, DPS-curcumin was recently synthesized and immobilized on the surface of NLs. Such NLs, designed as tracers of amyloid deposits, were found to strongly label abeta brain depositions *in vitro*, and *in vivo* [11]. In order to add a PEG-spacer between the lipid and curcumin moiety in the previously synthesized curcumin–lipid derivative, a commercially available DSPE-PEG2000-MAL functionalized lipid was reacted with 4-methoxytrityl-thiol (Mmt-SH), a compound already synthesized for the insertion of thiol-groups to sensitive molecules [19]. This DSPE-PEG2000-S-Mmt derivative (which serves as a precursor of DSPE-PEG2000-SH) was synthesized for the first time. The formation reaction of the DSPE-PEG2000-S-Mmt is quantitative (no by-products were detected) and proceeds fast in presence of DIPEA. After thiol deprotection DSPE-PEG2000-SH was reacted with curcumin, under Michael addition conditions, to give the corresponding DPS-PEG2000-CURC derivative. This new synthetic compound was efficiently inserted in NL membranes and by taking advantage of the two phenol-protons of the CURC moiety, the fluorescence intensity of the prepared NLs was substantially increased by adding DIPEA to DSPE-PEG2000-CURC (Table 2). This new chemical form of DSPE-PEG2000-CURC DIPEA salt was proven to efficiently label Aβ deposits in post-mortem tissues of AD patients (Figs. 2 and 3).

From a synthetic point of view, the current methodology can be used as an alternative technique to synthesize lipid–thiol preparations, after acidic cleavage of the Mmt-protecting group. Thus DSPE-PEG2000-S-Mmt may be considered as another precursor of DSPE-PEG2000-SH, besides DSPE-PEG2000-PDP [1,2-distearoyl-*sn*-glycero-3-phosphoethanolamine-N-[PDP (polyethylene glycol) −2000] (ammonium salt)] which is the main methodology currently applied [33,34]. This novel DSPE-PEG2000-S-Mmt thiol-protected lipid derivative can be safely stored, with its thiol-group efficiently protected from oxidation until usage, and when required, the Mmt-group can be cleaved under mild acidic conditions liberating the free thiol group.

Multifunctional NLs, having both Aβ-peptide and BBB targeting functionalities on their surface, were additionally prepared after immobilizing an anti-TfR MAb on DPS-PEG2000-CURC NLs, by reaction between pre-formed DPS-PEG2000-CURC NLs which

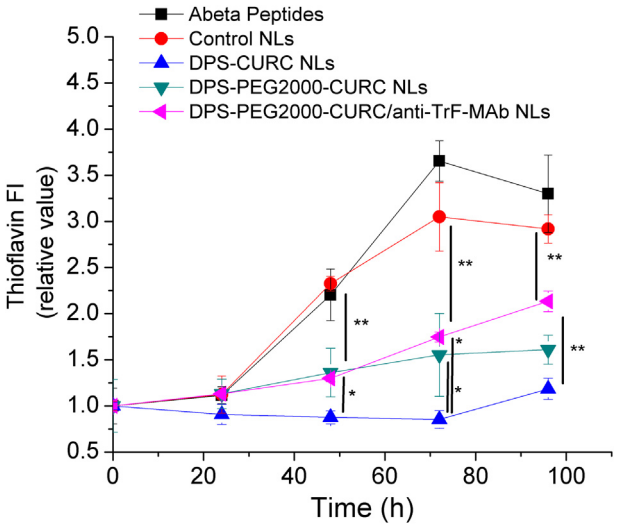

Fig. 4. Effect (measured as relative Thioflavin FI) of DPS-CURC; DPS-PEG2000-CURC; DPS-PEG2000-CURC/anti-TrF-MAb nanoliposomes (NLs) and control-liposomes on Aβ1-42 aggregation using ThT assay data (96-h time course). Each value is the mean value calculated from at least 3 different experiments and SD values are presented as bars. Statistical significant differences as presented in the graph (* for $p < 0.05$ and ** for $p < 0.01$).

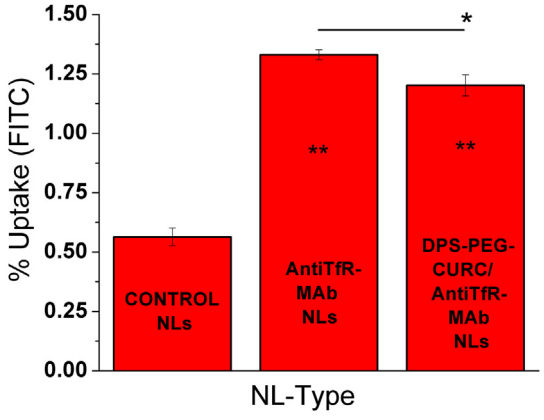

Fig. 5. Uptake of various types of nanoliposomes (NLs) by hCMEC/D3 cells, after incubation of 200 nmol lipid with 10^6 cells for 60 min at 37 °C. The uptake is expressed as the percent of NL-encapsulated FITC associated with the cells after the incubation was completed. Each value is the mean of at least 3 independent experiments carried out for each formulation and the SDs of means are presented. (*significant difference at $p < 0.05$; ** at $p < 0.01$). Stars in the bars are for differences between each specific sample and control NLs.

additionally incorporated DSPE-PEG2000-MAL in the membranes, and the thiolated MAb. By preparation of such multifunctional NLs, it was proven that the presence of the CURC-derivative on their surface does not reduce the MAb attachment yield, which was found to be similar (Table 1) to that measured previously for NLs that did not have other functionalities on their surface [22]. These multifunctional NLs were further demonstrated to strongly label Aβ deposits in post mortem tissues of AD patients (Figs. 2 and 3). Furthermore, it was proven that such multifunctional NLs can effectively inhibit Aβ1-42 aggregation almost as well as the DPS-CURC NLs (Fig. 4), indicating that the incorporation of the PEG spacer in the CURC-lipid derivative and the additional post-decoration of the NL-surface with the antibody, have only minimal effects on their anti-Aβ-activity.

Finally, the brain targeting capability of the multifunctional NLs was investigated in order to understand whether the presence of the CURC-derivative on their surface, modulates the ability of the antibody to interact with cell membrane receptors. For this, a BBB cellular model recently established as a good *in vitro* model for studying the brain-targeting potential of NLs (or in general nanoparticles) [22,32], was used. As demonstrated (Fig. 5), the brain targeting capability of the multifunctional NLs was only very slightly affected (<10% reduction of NL uptake by cells) by the presence of the CURC-derivative on their surface. Thereby, it is concluded that the novel multifunctional NLs formulated herein have indeed both functionalities in active form and may be used as AD theragnostic nanoformulations, to carry therapeutic and/or imaging agents to amyloid deposits in the brain.

Acknowledgements

This work was supported by the European Community's Seventh Framework Programme (FP7/2007-2013) under grant agreement n° 212043. The funding source had no role in the study design; the collection, analysis and interpretation of data; in the writing of the report; and in the decision to submit the article for publication. Authors are grateful to Dr. Mario Salmona (Mario Negri Institute, Milan, IT) for kindly providing the Aβ1-42 peptides, to Prof. K. Barlos (UPAT & CBL S.A., Patras, Greece), for kindly providing the 4-methoxytritylthiol, and to Dr. Pierre-Oliver Couraud (Inserm, Paris, FR) for the hCMEC/D3 cells.

Appendix A. Supplementary data

Supplementary data related to this article can be found at http://dx.doi.org/10.1016/j.ejmech.2014.04.050.

References

[1] American Psychiatric Association, Diagnostic and Statistical Manual of Mental Disorders, DSM-IV-TR, fourth ed., American Psychiatric Association, Washington, DC, 2000.
[2] B.T. Hyman, C.H. Phelps, T.G. Beach, E.H. Bigio, N.J. Cairns, M.C. Carrillo, D.W. Dickson, C. Duyckaerts, M.P. Frosch, E. Masliah, S.S. Mirra, P.T. Nelson, J.A. Schneider, D.R. Thal, B. Thies, J.Q. Trojanowski, H.V. Vinters, T.J. Montine, National Institute on Aging-Alzheimer's Association guidelines for the neuropathologic assessment of Alzheimer's disease, Alzheimer's & Dementia: the Journal of the Alzheimer's Association 8 (2012) 1–13.
[3] J. Hardy, Testing times for the "amyloid cascade hypothesis", Neurobiology of Aging 23 (2002) 1073–1074.
[4] T. Iwatsubo, A. Odaka, N. Suzuki, H. Mizusawa, N. Nukina, Y. Ihara, Visualization of A beta 42(43) and A beta 40 in senile plaques with end-specific A beta monoclonals: evidence that an initially deposited species is A beta 42(43), Neuron 13 (1994) 45–53.
[5] D.J. Selkoe, The cell biology of beta-amyloid precursor protein and presenilin in Alzheimer's disease, Trends in Cell Biology 8 (1998) 447–453.
[6] D.J. Selkoe, Alzheimer's disease: genes, proteins, and therapy, Physiological Reviews 81 (2001) 741–766.
[7] W.E. Klunk, H. Engler, A. Nordberg, Y. Wang, G. Blomqvist, D.P. Holt, M. Bergström, I. Savitcheva, G.F. Huang, S. Estrada, B. Ausén, M.L. Debnath, J. Barletta, J.C. Price, J. Sandell, B.J. Lopresti, A. Wall, P. Koivisto, G. Antoni, C.A. Mathis, B. Långström, Imaging brain amyloid in Alzheimer's disease with Pittsburgh Compound-B, Annals of Neurology 55 (2004) 306–319.
[8] D. Yanagisawa, T. Amatsubo, S. Morikawa, H. Taguchi, M. Urushitani, N. Shirai, K. Hirao, A. Shiino, T. Inubushi, I. Tooyama, In vivo detection of amyloid beta deposition using (1)F magnetic resonance imaging with a (1)F-containing curcumin derivative in a mouse model of Alzheimer's disease, Neuroscience 184 (2011) 120–127.
[9] M. Koronyo-Hamaoui, Y. Koronyo, A.V. Ljubimov, C.A. Miller, M.K. Ko, K.L. Black, M. Schwartz, D.L. Farkas, Identification of amyloid plaques in retinas from Alzheimer's patients and noninvasive in vivo optical imaging of retinal plaques in a mouse model, Neuroimage 54 (Suppl. 1) (2011) S204–S217.
[10] I. Lee, J. Yang, J.H. Lee, Y.S. Choe, Synthesis and evaluation of 1-(4-[(18)F] fluoroethyl)-7-(4'-methyl)curcumin with improved brain permeability for beta-amyloid plaque imaging, Bioorganic & Medicinal Chemistry Letters 21 (2011) 5765–5769.
[11] A.N. Lazar, S. Mourtas, I. Youssef, C. Parizot, A. Dauphin, B. Delatour, S.G. Antimisiaris, C. Duyckaerts, Curcumin-conjugated nanoliposomes with high affinity for Aβ deposits: possible applications to Alzheimer disease, Nanomedicine: Nanotechnology, Biology, and Medicine 9 (2013) 712–721.
[12] A.N. Begum, M.R. Jones, G.P. Lim, T. Morihara, P. Kim, D.D. Heath, C.L. Rock, M.A. Pruitt, F. Yang, B. Hudspeth, S. Hu, K.F. Faull, B. Teter, G.M. Cole, S.A. Frautschy, Curcumin structure-function, bioavailability, and efficacy in models of neuroinflammation and Alzheimer's disease, The Journal of Pharmacology and Experimental Therapeutics 326 (2008) 196–208.
[13] K. Ono, K. Hasegawa, H. Naiki, M. Yamada, Curcumin has potent anti-amyloidogenic effects for Alzheimer's beta-amyloid fibrils in vitro, Journal of Neuroscience Research (2004,Mar 15) 742–750.
[14] F. Yang, G.P. Lim, A.N. Begum, O.J. Ubeda, M.R. Simmons, S.S. Ambegaokar, P.P. Chen, R. Kayed, C.G. Glabe, S.A. Frautschy, G.M. Cole, Curcumin inhibits formation of amyloid beta oligomers and fibrils, binds plaques, and reduces amyloid in vivo, The Journal of Biological Chemistry 280 (2005) 5892–5901.
[15] S.G. Antimisiaris, P. Kallinteri, D.G. Fatouros, Liposomes, Drug Delivery, in: S.C. Gad (Ed.), Pharmaceutical Manufacturing Handbook: Production and Processes, John Wiley & Sons, Inc., Hoboken, NJ, USA, 2007, pp. 443–535.
[16] R.I. Jolck, L.N. Feldborg, S. Andersen, S.M. Moghimi, T.L. Andresen, Engineering liposomes and nanoparticles for biological targeting, Advances in Biochemical Engineering/Biotechnology 125 (2011) 251–280.
[17] L. Costantino, G. Tosi, B. Ruozi, L. Bondioli, M.A. Vandelli, F. Forni, Colloidal systems for CNS drug delivery, Progress in Brain Research 180 (2009) 35–69.
[18] S. Mourtas, M. Canovi, C. Zona, D. Aurilia, A. Niarakis, B. La Ferla, M. Salmona, F. Nicotra, M. Gobbi, S.G. Antimisiaris, Curcumin-decorated nanoliposomes with very high affinity for amyloid-β1-42 peptide, Biomaterials 32 (2011) 1635–1645.
[19] S. Mourtas, D. Gatos, V. Kalaitzi, C. Katakalou, K. Barlos, S-4-Methoxytrityl mercapto acids: synthesis and application, Tetrahedron Letters 42 (2001) 6965–6967.
[20] J.C. Dittmer, R.L. Lester, A Simple, Specific spray, for the detection of phospholipids on thin-layer chromatograms, Journal of Lipid Research 15 (1964) 126–127.
[21] J.C.M. Stewart, Colorimetric determination of phospholipids with ammonium ferro thiocyanate, Analytical Biochemistry 104 (1980) 10–14.
[22] E. Markoutsa, K. Papadia, A. Giannou, M. Spella, A. Cagnotto, M. Salmona, G.T. Stathopoulos, S.G. Antimisiaris, Mono and dually decorated nanoliposomes for brain targeting, in vitro and in vivo studies, Pharmaceutical Research (2014) (in press).
[23] H. Braak, E. Braak, Neuropathological stageing of Alzheimer-related changes, Acta Neuropathologica 82 (1991) 239–259.
[24] S.S. Mirra, A. Heyman, D. McKeel, S.M. Sumi, B.J. Crain, L.M. Brownlee, F.S. Vogel, J.P. Hughes, G. van Belle, L. Berg, The consortium to establish a registry for Alzheimer's disease (CERAD). Part II. Standardization of the neuropathologic assessment of Alzheimer's disease, Neurology 41 (1991) 479–486.
[25] Consensus recommendations for the postmortem diagnosis of Alzheimer's disease, The national Institute on aging, and Reagan Institute working group on diagnostic criteria for the neuropathological assessment of Alzheimer's disease, Neurobiology of Aging 18 (4 Suppl.) (1997) S1–S2.
[26] C. Manzoni, L. Colombo, M. Messa, A. Cagnotto, L. Cantu, E. Del Favero, M. Salmona, Overcoming synthetic Aβ peptide aging: a new approach to an age old problem, Amyloid: the International Journal of Experimental and Clinical Investigation: the Official Journal of the International Society of Amyloidosis 16 (2009) 71–80.
[27] B. Weksler, I.A. Romero, P.-O. Couraud, The hCMEC/D3 cell line as a model of the human blood brain barrier, Fluids and Barriers of the CNS 10 (2013) 16–26.
[28] E. Markoutsa, K. Papadia, C. Clemente, O. Flores, S.G. Antimisiaris, Anti-Aβ-MAb and dually decorated nanoliposomes: effect of Aβ1-42 peptides on interaction with hCMEC/D3 cells, European Journal of Pharmaceutics and Biopharmaceutics 81 (2012) 49–56.
[29] R.B. Greenwald, C.W. Gilbert, A. Pendri, C.D. Conover, J. Xia, A. Martinez, Water soluble taxol: 2′-poly(ethyleneglycol) ester prodrugs-design and in vivo effectiveness, Journal of Medicinal Chemistry 39 (1996) 424–431.
[30] A. Mukherjee, T.K. Prasad, N.M. Rao, R. Banerjee, Haloperidol-associated stealth liposomes. A potent carrier for delivering genes to human breast cancer cells, The Journal of Biological Chemistry 280 (2005) 15619–15627.

[31] M. Taylor, S. Moore, S. Mourtas, A. Niarakis, F. Re, C. Zona, B. LaFerla, F. Nicotra, M. Masserini, S.G. Antimisiaris, M. Gregori, D. Allsop, Effect of curcumin-associated and lipid ligand-functionalized nanoliposomes on aggregation of the Alzheimer's Aβ peptide, Nanomedicine: Nanotechnology, Biology, and Medicine 7 (2011) 541–550.
[32] E. Markoutsa, G. Pampalakis, A. Niarakis, I.A. Romero, B. Weksler, P.-O. Couraud, S.G. Antimisiaris, Uptake and permeability studies of BBB-targeting immunoliposomes using the hCMEC/D3 cell line, European Journal of Pharmaceutics and Biopharmaceutics: Official Journal of Arbeitsgemeinschaft Fur Pharmazeutische Verfahrenstechnik e.V 77 (2011) 265–274.
[33] S.A. DeFrees, L. Phillips, L. Guo, S. Zalipsky, Sialyl Lewis × liposomes as a multivalent ligand and inhibitor of E-selectin mediated cellular adhesion, Journal of the American Chemical Society 118 (1996) 6101–6104.
[34] S. Zalipsky, N. Mullah, J.A. Harding, J. Gittelman, L. Guo, S.A. DeFrees, Poly(-ethylene glycol)-grafted liposomes with oligopeptide or oligosaccharide ligands appended to the termini of the polymer chains, Bioconjugate Chemistry 8 (1997) 111–118.